Contents list available at CBIORE journal website

International Journal of Renewable Energy Development

Journal homepage: https://ijred.cbiore.id

Research Article

Optimization of energy efficiency and purge strategy of an open-cathode PEMFC stack with a dead-end anode configuration

Tan-Thich Do[a*], Trung-Kien Vi[a], Phuoc-Dong Doan[b]

[a]*Department of Electrical and Mechatronics, Lac Hong University, Vietnam*

[b]*Department of Mechanical Engineering, School of Engineering, King Mongkut's Institute of Tecnhnology Ladkrabang, Bangkok, Thailand*

Abstract. Nowadays, proton exchange membrane fuel cells (PEMFCs) are acknowledged as promising energy solutions toward reaching net-zero emissions by 2050 due to their highlighted properties, such as high energy efficiency, high power density, low operating temperature, fast start-up, and zero emissions. To enhance electrochemical reactions and improve hydrogen utilization, the dead-end anode (DEA) configuration was employed to investigate the voltage and energy efficiency of an open-cathode PEMFC stack (100 W-20 cells) at optimal fan speed under varying purge intervals and operating current load levels with the step-by-step method. The hydrogen purge operation optimization was proposed by fitting experimental data and deriving the governing equation, considering voltage stability and hydrogen consumption. The results show that when the operating current and purge interval increased, the stack voltage decreased owing to impurities, water, and nitrogen buildup in the flow field anode channel. At optimal purge intervals of 540, 360, 280, and 60 s, the energy efficiency was achieved at 45.55%, 45.31%, 43.11%, and 35.05%, respectively. Compared to a previous study, these values represent increases of 25.22%, 12.91%, 9.15%, and 2.09% for operating currents of 1, 3, 5, and 8 A, respectively. These improvements were achieved by optimizing the fan speed, purge interval, and microcontroller unit power consumption. At a low load level of 1 A, the voltage decay rate decreased from 0.45 mV s^{-1} to 0.07 mV s^{-1}, allowing for stable cell performance and higher hydrogen utilization at longer purging intervals. However, at higher load levels, both the voltage change of the stack and the voltage decay rate of the stack increased significantly compared to the 1 A case, with a steeper slope corresponding to higher current levels. This indicated that at higher reaction rates, the amount of water generated from the oxygen reduction reaction increases significantly. Consequently, the back diffusion phenomenon from the cathode to the anode, along with nitrogen buildup, leads to adverse conditions such as anode channel flooding and fuel starvation. This study provides meaningful insights into optimizing the energy efficiency of open-cathode PEMFC stacks across various load levels and purge operations.

Keywords: dead-end anode, energy efficiency, purge strategy, purge operations, purge interval, purge duration, open-cathode PEMFC stack, voltage stability, hydrogen utilization.

Received: 14th Dec 2025; Revised: 16th March 2026; Accepted: 10th April 2026; Available online: 30th April 2026

1. Introduction

Nowadays, with the decline of fossil fuel resources and the increasing impacts of greenhouse gases, proton exchange membrane fuel cells (PEMFCs) emerge as an appealing alternative to the conventional engine because PEMFCs have attractive properties such as a lack of moving parts, less noise, zero emissions, high efficiency, high density, and fast start-up (Abdelkareem *et al.* 2021; Barbir *et al.* 2012). Additionally, it was applied to stationary power, portable stations (Wilberforce *et al.* 2016), energy storage systems (Paul *et al.* 2016), unmanned aerospace vehicles (UAVs) (Wang *et al.* 2020), unmanned underwater vehicles (UUVs) (Sezgin *et al.* 2022), automobiles (Wilberforce *et al.* 2017), railways (Lee *et al.* 2024), and maritime (Van Biert *et al.* 2016). Therefore, PEMFCs have the potential to significantly reduce reliance on fossil fuels while simultaneously minimizing the environmental impact associated with traditional energy systems. As such, they are regarded as a crucial technology for contributing to net-zero emissions by 2050 (Khokhar *et al.* 2023).

Generally, the open-cathode PEMFC stack uses an electric fan to provide oxygen from the atmosphere. Additionally, the electric fan was used to cool the heat generated from the stack's reaction in the electrochemical cell. Therefore, the PEMFC stack's temperature plays a crucial role in the performance. (Zeng *et al.* 2019) examined the stack performance under various load levels and fan speeds via the duty cycle ratios. Their result shows that fan speed significantly impacted the voltage, distribution of the temperature, voltage uniformity, and energy efficiency. (Sasmito *et al.* 2012) designed the stack and evaluated the performance under varying fan configurations. They concluded that the fan configuration, including the power of the fan, connected in series or single fans, and the type of fans, affected the performance. (Yu *et al.* 2023) conducted an experiment to investigate the stack performance and self-regulation under varying electric fan operating conditions, including the suction mode and blow mode. They revealed that the suction mode is superior to the blow mode in the mechanism of self-regulation capability. Similarly, (Ling *et al.* 2016) evaluated the stack performance with the drawing and blow modes. They indicated that the performance was improved by

* Corresponding Author
Email: dotanthich@lhu.edu.vn (T.T.Do)

https://doi.org/10.61435/ijred.2026.62153
ISSN: 2252-4940/© 2026.The Author(s). Published by CBIORE

16% when the drawing air mode was used in their system. To optimize the stack temperature, (Yu *et al.* 2024) proposed a control strategy with a constraint-generalized predictive algorithm for the rated power stack of 1000 W. The result provides a highlight control strategy to achieve the highest performance stack in the kW class. (Zhao *et al.* 2021) designed the fuel cell stack and spoiler in the fan system to investigate the voltage, distribution of the temperature, and voltage uniformity with an 11-cell under different fan mechanisms, including spoiler-drawing air mode, spoiler-blowing air mode, and the distance between the stack and fan. The results show that the performance was increased with a fan distance of 80 mm for the spoiler-drawing air mode by 7.9% and spoiler-blowing by 7.3%, respectively. (Kandidayeni *et al.* 2019) proposed a fan speed control strategy to optimize the system efficiency using the fuzzy logic technique. The results show that the system efficiency improved from 13% to 16%. Recently, (Chen *et al.* 2019) experimented to evaluate the voltage under the blow mode and exhaust mode for the stack with 19 cells. They revealed that the performance and voltage uniformity with the blow mode are superior to the exhaust mode. (Song *et al.* 2020) experimented to discuss the stack performance with 60 W, 19 cells, and self-regulation under varying air flow rates. They indicated that the stack temperature ability was regulated when the load level was changed. (Guo *et al.* 2024) experimented to analyze the dynamic response of temperature and stack voltage. The result indicated that the fan's duty cycle of 0.4 is suitable for low load current, and 0.6 at medium and high current. (Zhou *et al.* 2023) examined the parameters of fans on the performance under load currents and fan duty cycles. They concluded that the fan parameters should be chosen depending on the applications. (Mus *et al.* 2025) experimented to evaluate the effect of the air ambient on the open-cathode PEMFC performance. They indicated that the best power of the fuel cell was achieved at a relative humidity of 75% and a temperature of 35 ^{o}C.

To save the hydrogen utilization and enhance the effectiveness of hydrogen utilization, enhance the electrochemical reaction, the dead-end anode (DEA) configuration and recirculation configuration were used in the system. The recirculation configuration used the solenoid valve, pump, and ejector, resulting in increasing system cost, complex system, complicated strategy control, and consumption of more energy (Kurniaa *et al.* 2019; Chen *et al.* 2013). The dead-end configuration just used only a purge valve to block the hydrogen gas at the outlet pipe, resulting in a simple system, reduced cost, and easy control, consuming less energy. Thus, the DEA mode presents a simplified approach to optimize hydrogen utilization (Kurniaa *et al.* 2019; Yu *et al.* 2014). In the DEA mode, performance will decrease gradually due to flooding and hydrogen starvation (Baumgartner *et al.* 2008; Abbou *et al.* 2015; Ohs *et al.* 2011). As the solenoid valve is opened, the impurities, water, nitrogen diffusion from the cathode to the anode, and unreacted hydrogen are exhausted to the ambient environment, and the performance is recovered immediately (Lee *et al.* 2009; Meyer *et al.* 2016; Mokmeli *et al.* 2010). Despite its efficiency advantages, DEA can negatively affect the lifespan of critical components, especially the membrane and gas diffusion layer. Indeed, (Hu *et al.* 2016) pointed out that flooding results not only from water diffusion but also from nitrogen accumulation, which blocks hydrogen from reaching the reaction zone, causing hydrogen starvation further downstream. (Pei *et al.* 2022) researched the formation of liquid water in a transparent PEMFC; the buildup of water in the anode channel is shown to obstruct hydrogen transport, increasing the risk of physical degradation, especially under dynamic operating conditions. The local degradation in PEMFCs operating under DEA configuration was investigated by (Yang *et al.* 2020). Their study revealed that flooding conditions can lead to increased mechanical stress on the components of the fuel cell, particularly negatively affecting the catalyst layers and membrane. Therefore, the selection of the purging interval is crucial to last a long time of membrane duration and enhance energy efficiency (Baz *et al.* 2024). The water transport in the stack using the visualization method was studied by (Rahimi-Esbo *et al.* 2020). They indicated that the water accumulation can be caused by the non-uniformity of the volatge reduce performance. While (Li *et al.* 2024) used a visualization combined with artificial intelligence to recognize the water in the fuel cells. (Xu *et al.* 2025) proposed the purge control strategy to improve the performance of the fuel cell. They revealed that the PSO-BP-PID control strategy to achieve high hydrogen utilization of 99.7%. (Shi *et al.* 2025) optimized the fuel cell performance and shutdown purge strategy based on machine learning. Their results show that the effectiveness of the optimization strategy optimized conditions increases the high-frequency resistance value by 0.79 mΩ. (Xiao *et al.* 2025) studied the performance of the open-cathode PEMFC stack in the DEA mode. Their results revealed that the cyclic exhaust can reduce the degradation of the fuel cell voltage. (Liu *et al.* 2026) studied the anode internal purge on the open-cathode PEMFC. Their results indicated that the system efficiency improved from 25.71% to 48.29%.

The nitrogen gas diffusion phenomenon from the cathode to the anode leads to voltage degradation during the DEA configuration. (Baik *et al.* 2008; 2011) studied the nitrogen crossover phenomenon in the fuel cell stack. Their results show the nitrogen diffusion under varying operating conditions. (Müller *et al.* 2010) created a model to estimate the nitrogen buildup in the stack channel. They indicated that the nitrogen caused the voltage performance and should be removed, considering the voltage decay and hydrogen utilization. Similarly, (Kocha *et al.* 2006) studied the characterization of gas crossover and developed a model to estimate nitrogen accumulation. Their model was validated by experiment, and they concluded that the nitrogen accumulated around 5% to 10% at the anode outlet. (Ahluwalia *et al.* 2007) discussed the nitrogen diffusion and accumulation in the anode channel in the stack for the automotive 90-kW. Their results discussed in detail the nitrogen gas accumulation under various operating conditions. (Meyer *et al.* 2014) investigated the nitrogen buildup in the channel during the DEA mode using thermal imaging and electrochemical impedance spectroscopy methods. The result shows that there is higher nitrogen accumulation at higher load levels. (Manokaran *et al.* 2011) experimented to investigate the inert gas during the DEA mode. They revealed that the inert gas percentage occupied 57%, 45%, and 35% under load currents of 600, 300, and 150 mA cm^{-2}. (Yang *et al.* 2025) predicted the nitrogen content at the anode side and proposed the purge strategy to optimize the fuel cell performance. Their results show that the energy efficiency improved by 0.5-1%.

In summary, the temperature and hydrogen utilization of the open-cathode PEMFC stack impacted a majority of the stack's performance and energy efficiency during its operation. Therefore, the optimization of the purge valve operation and the electric fan speed play a key role in optimizing the performance and energy efficiency of the stack. In our previous publication (Do *et al.* 2024), the fan speed was optimized under various fan duty factors and operating currents. On the other hand, the purge operation holds significant importance in removing the water, impurities, and nitrogen to recover the performance and save the hydrogen utilization. Frequently purging leads to more

unreacted hydrogen being purged, resulting in wasted hydrogen and consuming more auxiliary power, while longer purging leads to voltage deterioration. Therefore, the purge strategy should consider voltage stability and hydrogen utilization. The objective of this study was investigated and evaluated the stack performance and energy efficiency under varying purge operations at optimal fan speed. Additionally, the hydrogen purge strategy was proposed to optimize energy efficiency, considering voltage stability and hydrogen consumption.

2. Experimental setup

2.1. Experimental setup

Fig. 1 depicts the scheme of an experimental setup for this research. It consists of the supplied hydrogen gas components, the stack of open-cathode PEMFC integrated with an electric fan, a purge valve, a hydrogen supply valve, sensors, recording devices, and an electric load machine. A commercial stack of open-cathode PEMFC (MT18S248-100, Horizon Fuel Cells Technologies, Singapore) was used for the experiment. Additionally, Table 1 details the technical characteristics of the open-cathode PEMFC stack.

At the anode side, dry hydrogen (99.999%) was fed and depressurized using a pressure-reducing valve (IR4004, Parker, Taiwan). Additionally, a pressure regulator (R06-221, Norgren, Mexico) was employed to maintain a stable hydrogen inlet pressure. A pressure gauge (Wika Model 131.11 Bourdon, Netherlands) was installed to intuitively display the hydrogen inlet pressure. A check valve (SS-4C 521571001, Swagelok, USA) was used to prevent backpressure from the hydrogen in a stack from entering the hydrogen mass flow meter during purge valve operation. To enhance the electrochemical reaction and achieve cost-effective hydrogen utilization, the solenoid valve, which was called the purge valve, was used to block the hydrogen outlet during DEA mode. At the cathode side, an axial electrical fan, integrated into the stack, was employed to dissipate heat generated by the stack and supply air from the environment.

The electric load machine (PLZ164WA, Kikusui, Japan) was utilized to apply load levels to the stack during the experimental process. The direct current (DC) power source (U8001A, Keysight, USA) was employed to supply electrical power to the auxiliary equipment. In this research, a microcontroller unit (MCU) was designed and fabricated to control the auxiliary components, including the hydrogen supply valve, purge valve, and electric fan. The specifications of the MCU are tabulated in Table 2. Furthermore, the control program was developed using the MATLAB/Simulink software environment and embedded into the MCU. A hydrogen mass flowmeter (Alicat, SLPM10-D/5M-M, USA) was installed to determine the flow rate of hydrogen. A shunt current sensor (SH-0010A-50mV, CPU Co., Ltd, Taiwan) was used to measure the auxiliary currents and stack currents. To monitor the stack temperature, a thermocouple (WTC-TT-T-36, IOThrifty, USA) was placed at the center of the stack. Data acquisition was managed using a data acquisition card (DAQ, NI 1991, USA), which communicated with and processed signals via LabVIEW software. The DAQ recorded key parameters, including the hydrogen flow rate, stack voltage, stack current, auxiliary current, and stack temperature.

The power consumption of the MCU of 1 W in this study, compared to previous studies using the commercial NI my-RIO (Do *et al.* 2024), is 6 W for the NI my-RIO. Therefore, the improvement of the MCU in this study significantly contributed to reducing the auxiliary power consumption, resulting in energy efficiency increased.

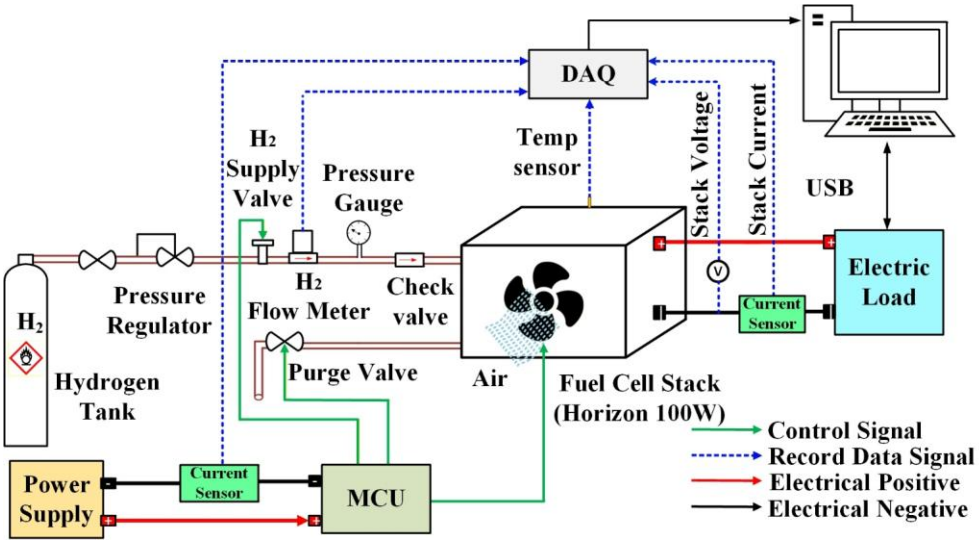

Fig. 1 Experimental setup schematic in this study

Table 1
Technical characteristics of the open-cathode PEMFC stack

Specifications	Values
Cell number	20
Cell activation area	22.5 (cm^2)
Nominal output power	100 W
Maximum power	9.3 A @ 12 V
Dimensions of the stack	118 × 104 × 94 mm
Weight of stack	1290 ± 50 g
Inlet pressure	0.45 – 0.5 bar

Table 2
Specifications of the MCU in this study

Specification	Description
Host architecture	AVR/ATMega2560
Input voltage	12 V
Clock speed	16 MHz
Dimension compact	100 × 80 × 20 mm
Weight	150 g

2.2 Experiment procedure

Before performing tests in DEA mode to investigate the stack performance and energy efficiency under varying load levels and purge intervals, the fuel cell stack underwent a one-hour activation process at a constant load of 4 A. This activation aimed to achieve high and stable performance by humidifying the membrane and removing impurities. Subsequently, water and impurities were expelled by controlling the hydrogen flow rate using a purge valve with a continuous on-off signal, ensuring optimal conditions before starting the experiments.
The electric fan speed significantly influenced the stack's performance, as it not only supplied air from the environment but also dissipated heat generation from the electrochemical reactions of the fuel cell stack. The electric fan speed was managed using the pulse width modulation (PWM) technique, where the duty cycle ratio determined the fan's operating speed. The duty cycle ratio was defined as follows (Wang *et al.* 2010):

$$D_{fan} = \frac{T_{on}}{T_{cycle}} \quad (1)$$

Where T_{on} and T_{cycle} refer to the pulse width time and period time of one cycle, respectively.

A lower fan duty cycle ratio, resulting in reduced fan speed, may lead to insufficient airflow or inadequate dissipation of heat generated by the fuel cell stack. Conversely, a higher fan duty cycle ratio increases fan speed but also results in higher power consumption. Therefore, determining the optimal fan speed is crucial for efficient stack operation. In our previous study (Do *et al.* 2024), energy efficiency was evaluated under various fan duty cycle ratios. The optimal duty cycle ratio was found to be 20% at low and medium operating currents. For high operating current densities, the optimal duty cycle ratio increased to 40%, as the higher fan speed was necessary to provide adequate airflow and dissipate the heat generated under high load conditions.

During stack operation in DEA mode, purge operations significantly influenced energy efficiency. The solenoid valve operation status is illustrated in Fig. 2(a). Notably, the purge duration represents the period during which the solenoid valve remains open, while the purge interval denotes the period during which the solenoid valve is closed. According to theory, a higher operating current level results in higher water generation (O'Hayre *et al.* 2016). Therefore, the purge interval was set low value to remove the water vapor in the flow field channels early and supply fresh hydrogen gas at a high operating current level. In this research, the purge duration was fixed at 0.1 s, and the purge interval was varied in steps of 180, 60, 40, and 20 s, corresponding to operating currents of 1 A, 3 A, 5 A, and 8 A, respectively. Stack performance and energy efficiency were evaluated under these varying purge intervals and operating currents. The energy efficiency was calculated based on Eq. (2):

$$\eta_{LHV} = \frac{\int P_{net}(t)dt}{LHV \int \dot{m}_{H_2}(t)dt} = \frac{\int (P_{stack}(t) - P_{aux}(t))dt}{LHV \int \dot{v}_{H_2}(t)dt} \quad (2)$$

Where: P_{net}, P_{stack}, P_{aux}, LHV and $\dot{v}_{H_2}$ denote the net power output, power of the open-cathode fuel cell stack, auxiliary

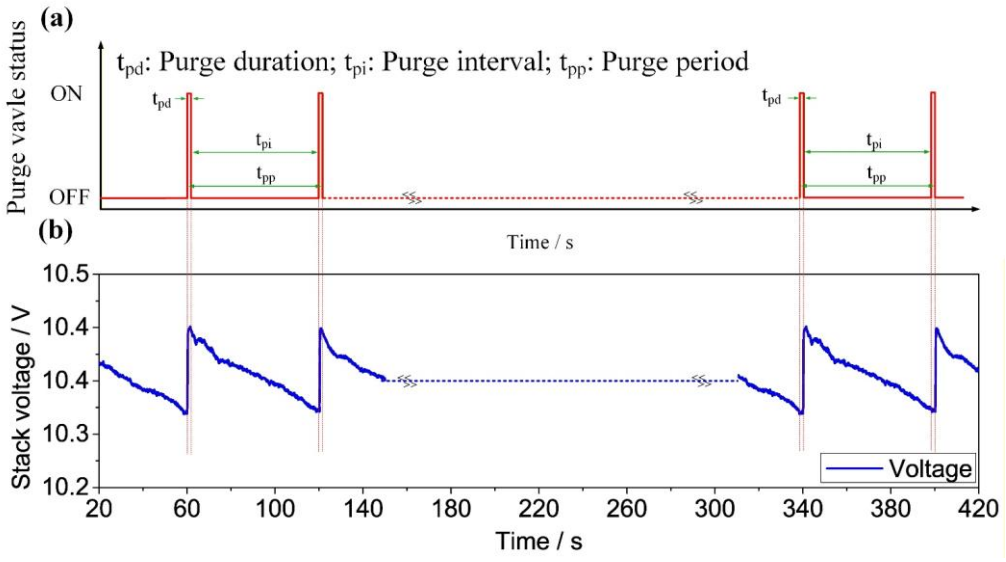

Fig. 2 (a) Description of the purge process; (b) Purge index

consumption power, hydrogen's lower heating value ($LHV = 241\ kJ\ mol^{-1}$), and volume of hydrogen flow rate, respectively. The stack power in Eq. (2) was determined following Eq. (3):

$$\int P_{stack}(t)dt = \int (I_{stack}(t) \times V_{stack}(t)\, dt \tag{3}$$

Where: I_{stack} and V_{stack} denote the stack current and stack voltage, respectively.

Additionally, the auxiliary power consisting of the power consumption of the purge valve, hydrogen supply valve, electric fan, and MCU can be determined following Eq. (4):

$$\begin{aligned}\int P_{aux}(t)dt = \int (&P_{pv}(t) + P_{Hsp}(t) + P_{Fan}(t) \\ &+ P_{MCU}(t))dt \\ &= \int (I_{aux}(t) \times V_{aux}\,(t))dt\end{aligned} \tag{4}$$

Where: P_{Pv}, P_{Hsp}, P_{Fan}, and P_{MCU} represent the power consumption of the purge valve, hydrogen supply valve, electric fan, and MCU, respectively. In addition, I_{aux} V_{aux} denote the auxiliary current and auxiliary voltage, respectively.

The hydrogen consumption flow rate depended on the load levels during stack operation in DEA mode. Hydrogen consumption comprised two components: hydrogen utilized by the fuel cell stack owing to the reaction of the electrochemical and hydrogen wasted, which was exhausted during the purging process. It can be calculated using Eq. (5):

$$\int \dot{v}_{H_2}(t)dt = \int (\dot{v}_{H_{2,fc}}(t) + \dot{v}_{H_{2,pp}}(t))\, dt \tag{5}$$

Where: $\dot{v}_{H_{2,fc}}$is the flow rate of the hydrogen consumption for the electrochemical reaction of the stack, and $\dot{v}_{H_{2,pp}}$ represents the wasted hydrogen consumption flow rate owing to the purging process.

The flow rate of the hydrogen consumption for the electrochemical reaction of the stack depended on the load level and the number of cells. It was determined by Eq. (6):

$$\int \dot{v}_{H_{2,fc}}(t)dt = \int \left(\frac{I_{stack}(t) \times n}{2F}\right) dt \tag{6}$$

Where: F and n denote Faraday's constant ($F = 96485\ C\ mol^{-1}$), and the cell number in the stack, respectively. Additionally, the wasted hydrogen consumption flow rate due to the purging process occurred in the purge valve opened and can be determined by Eq. (7):

$$\int \dot{v}_{H_{2,pp}}(t)\, dt = \int \frac{5140}{3600} \times K_v \times \sqrt{\frac{(p_a - p_0)p_0}{\rho T_{stack}(t)}}\, dt \tag{7}$$

Where: K_v, p_a, p_0, ρ, and T_{stack} represent the purge valve characteristic, anode inlet pressure, anode outlet pressure at the time the purge valve is opened, density of hydrogen, and stack temperature, respectively.

During the stack operation with the DEA configuration, the stack voltage is impacted by the purge interval. To evaluate stack voltage variations, the stack voltage change and stack voltage decay rate were regarded in this study. They were described and shown in Fig. 2(b). The stack voltage change (V_{sc}) and stack voltage decay rate (V_{dc}) was determined following Eq. (8) and Eq. (9), respectively:

$$V_{sc}(i) = V(i)_{max,ap} - V(i)_{min,dp} \tag{8}$$

$$V_{dc}(i+1) = \frac{V(i)_{max,ap} - V(i+1)_{min,bp}}{T_{p(i)}} \tag{9}$$

Where: $V(i+1)_{min,bp}$ $V(i)_{max,ap}$, and $\mathrm{V(i)_{min,dp}}$ are the minimum stack voltage before the next purging at the end of the (i +1)th cycle, the highest stack voltage after a previous purging at i -th purge, and the lowest stack voltage during the purge process, respectively; $T_{p(i)}$ denotes the purge interval of the solenoid valve, and i is the summation index.

2.3 Hydrogen purge strategy and optimization of energy efficiency

During the stack operation with a DEA mode, as the solenoid valve was opened, the unreacted hydrogen gas, along with impurities and water were exhausted into the atmosphere. Therefore, the possible maximum purging times number (N) over the purge period, which was finished to discharge the gas into the outside when the solenoid valve was opened, can be determined as Eq. (10):

$$N = \frac{\Delta t_{fc}}{t_{pp}} = \frac{\Delta t_{fc}}{t_{pi} + t_{pd}} \tag{10}$$

Where: Δt_{fc} is the total of open-cathode PEMFC stack operation time, t_{pi} is the purge interval, and t_{pd} is the purge duration. All of the values above are in units of seconds (s). N should integer number and rounded down based on experiments.

The total of pure time possible maximum (τ_p) in seconds (s) can be defined based on the possible maximum purging times number (N) and (t_{pd}) purge duration as follows in Eq. (11):

$$\tau_p = N \times t_{pd} \tag{11}$$

The voltage of the stack progressively decreased during the DEA configuration. The primary reason was determined to be the impurity, water generation occupying the channels due to the back diffusion phenomenon, and nitrogen buildup due to diffusion from the cathode to the anode, leading to a decline in the electrochemical reaction area. To evaluate the voltage stability, the average voltage degradation was considered during open-cathode PEMFC stack operation with DEA mode in this study. In addition, lower values of the average voltage degradation were considered better. In other words, achieving stable cell voltage output, which can be evaluated by low average voltage degradation, was desirable for cell voltage stability. The average voltage degradation (in mV) can be determined by the following Eq. (12):

$$\bar{V}_d = \frac{1}{N}\sum_{i=1}^{N}\left(V_{t_{ap}^{i}} - V_{t_{bp}^{i+1}}\right) \tag{12}$$

Where: $V_{t_{ap}^{i}}$, $V_{t_{bp}^{i+1}}$, N, and i denote the stack voltage in mV (after previous purging) at the beginning of the new cycle (i+1)th, the stack voltage in mV (before next purging) at the end of the (i+1)th cycle, the possible maximum number of purging times, and index of summation, respectively.

To evaluate the reliability of the governing equation, the mean absolute percentage error (MAPE) was employed and expressed following Eq. (13). The governing equation was fitted through an optimal purge interval under varying load levels with a high regression (R^2) value of 1.0 and a low MAPE:

$$MAPE = \sum_{i=1}^{N}\left(\frac{|t_{pi_e} - t_{pi_p}|}{t_{pi_e}}\right)\frac{1}{N} \times 100\% \quad (13)$$

Where: t_{pi_e}, t_{pi_p}, and N denote the purge interval from the experiment, the purge interval from the proposal in this study, and the number of load levels.

3. Results and discussion

3.1 Impact of purge interval on stack performance under load levels

The voltage of the open-cathode PEMFC stack during DEA configuration operation was analyzed under varying operating currents and purge intervals, where the purge intervals represent the duration for which the purge valve remains closed in this study. Fig. 3 illustrates the stack voltage variation at an operating current of 1 A under different purge intervals. It was seen that as the purge interval increased, the stack voltage decreased during the purge valve closed period. At a low operating current of 1 A, with purge intervals of 180 s and 360 s, the stack voltage gradually declined over a 40-minute experimental duration, as described in Fig. 3(a) and 3(b). However, the voltage performance decreased slightly more with a 180 s purge interval than with a 360 s interval. This occurred because the more frequent opening of the purge valve led to greater hydrogen losses, resulting in less stable stack voltage. As the purge interval increased to 540 s, the stack voltage appeared stable, as described in Fig. 3(c). This was attributed to the optimal timing of purge valve operations, ensuring appropriate hydrogen release and stable voltage with minimal hydrogen wastage. Consequently, a purge interval of 540 s was identified as the optimal interval at an operating current of 1 A. In contrast, at a purge interval of 720 s, the stack voltage performance deteriorated after the 65th minute, as shown in Fig. 3(d). This was caused by excessive water accumulation and potential carbon catalyst degradation. In general, the stack voltage performance at a low operating current of 1 A remained relatively stable and declined only slightly as the purge interval increased, owing to limited water buildup in the channels. Additionally, the stack temperature was relatively low and did not reach the optimal range because the low operating current generated insufficient heat.

When the open-cathode fuel cell stack was elevated to a higher load level of 3 A, the stack voltage demonstrated a gradual and notable increase at purge intervals of 60 and 180 s. This improvement can be attributed to the higher heat generated by the stack, which enhanced the electrochemical reactions, as mentioned in Fig. 4(a) and 4(b). In addition, the voltage remained relatively stable with minor reductions during

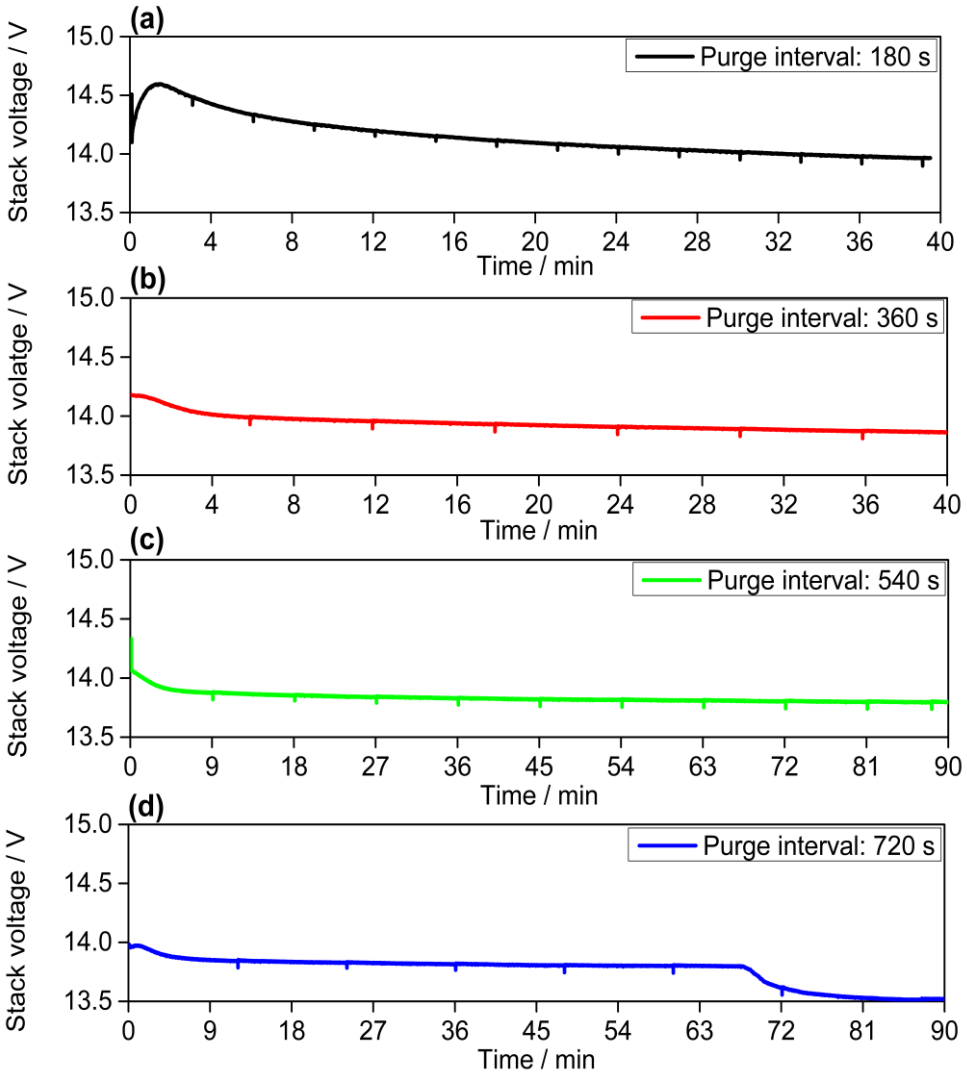

Fig. 3 Voltage of stack performance under varying purge intervals at an operating current of 1 A: (a) 180 s; (b) 360 s; (c) 540 s; and (d) 720 s

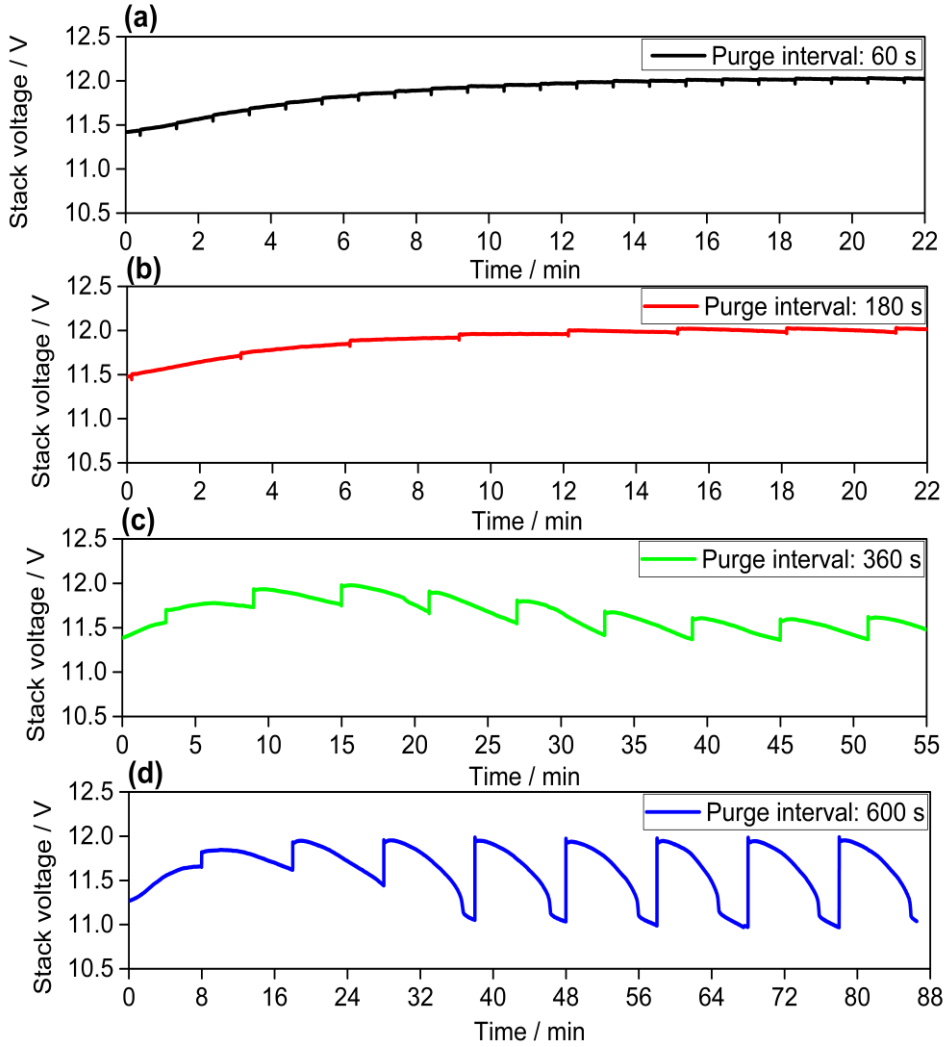

Fig. 4 Voltage of stack performance under varying purge intervals at an operating current of 3 A: (a) 60 s; (b) 180 s; (c) 360 s; and (d) 600 s

each cycle once the stack temperature reached a steady state. This behavior was explained by the frequent opening of the solenoid valve, which effectively removed water, impurities, and nitrogen buildup, allowing for prompt recovery of stack voltage performance. When the purge interval was increased to 360 s, the stack voltage progressively declined during the purge valve closed period, with a voltage loss of approximately 0.18 V per cycle, as depicted in Fig. 4(c). This voltage drop was caused by the impurities, water, and nitrogen accumulation in the anode channel, which reduced the effective activation area of the fuel cell. At a further increased purge interval of 600 s, the stack voltage performance deteriorated significantly, with a voltage loss of approximately 1 V recorded during DEA mode operation, as shown in Fig. 4(d). The closed purge valve extension led to excessive water, impurities, and nitrogen buildup, further diminishing the active cell area and negatively affecting the stack's performance.

At the current of 5 A, the stack voltage performance showed a gradual and slight decrease during the purge valve closed period at purge intervals of 80 and 60 s. This behavior is similar to the trends observed at lower load levels. The water, impurities, and nitrogen were expelled effectively due to the short purge intervals and periodic purging, allowing for prompt recovery of stack voltage performance, as described in Fig. 5(a) and 5(b). However, when the purge interval increased to 280 and 360 s, the stack voltage performance declined significantly, with voltage losses of approximately 1.2 V and 1.5 V during DEA mode operation, respectively. At this load level, the optimal purge interval was identified as 280 s, considering both the number of purge events and the stability of the stack voltage. Specifically, while shorter purge intervals ensured stable voltage performance, they resulted in higher hydrogen wastage. Conversely, longer purge intervals reduced hydrogen waste but caused voltage instability. Thus, the optimal purge interval in this study balances stable voltage performance and hydrogen utilization, which was found at 280 s, as depicted in Fig. 5(c). When the purge interval was further increased to 360 s, the stack voltage performance deteriorated significantly, as shown in Fig. 5(d). This reduction can be explained by the excessive buildup of impurities, water, and nitrogen at the anode flow field channel, resulting in a reduced electrochemical reaction area and negatively impacting stack performance.

As the stack operation at a high load of 8 A, the voltage remained stable with short purge intervals of 20 and 40 s, as described in Fig. 6(a) and 6(b). This phenomenon is caused by the frequent opening of the solenoid valve, which facilitates the continuous removal of impurities, water, and nitrogen buildup from the anode flow field channel. Consequently, more unreacted hydrogen was expelled. As the purge interval increased to 60 s, the stack voltage gradually decreased during DEA mode; however, the voltage did not decline sharply, and the purge process remained effective, as shown in Fig. 6(c).

Therefore, a purge interval of 60 s was considered optimal due to voltage stability and reduced unreacted hydrogen. As the fuel cell stack operated with a purge interval of 120 s, the voltage deteriorated significantly, as more water, nitrogen, and impurities accumulated in the anode channel, reducing the activation electrochemical reaction area, as depicted in Fig.

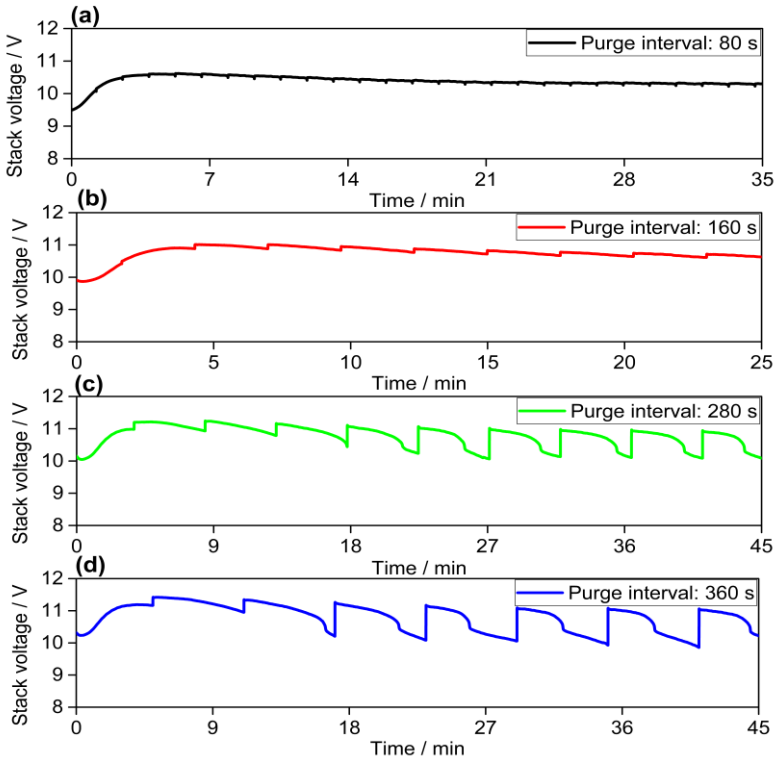

Fig. 5 Voltage of stack performance under varying purge intervals at an operating current of 5 A: (a) 80 s; (b) 160 s; (c) 280 s; and (d) 360 s

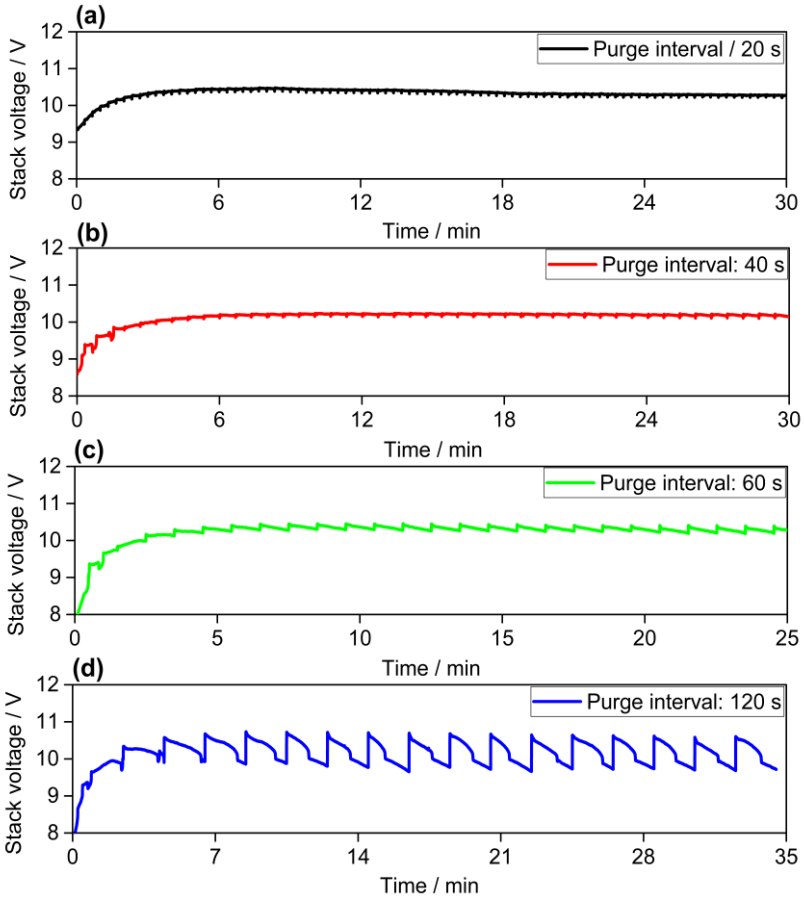

Fig. 6 Voltage of stack performance under varying purge intervals at an operating current of 8 A: (a) 20 s; (b) 40 s; (c) 60 s; and (d) 120 s

6(d). This buildup of nitrogen, water, and impurities at high operating current obstructed proton diffusion across the membrane and hindered hydrogen transport to the active electrochemical sites. Water buildup led to flooding downstream of the anode channel, reducing the contact area between hydrogen and the surface of the catalyst, thus reducing the efficiency of the electrochemical reaction. As water filled the gas channels and the catalyst layer pores, it displaced hydrogen, limiting its access to the catalyst surface and making the reaction less effective.

3.2 Impact of load levels on stack performance

Fig. 7(a), (c), (e), and (g) show the stack voltage during stable operation at various operating currents and optimal purge intervals. It can be observed that as the load levels increased, the stack voltage decreased due to higher overpotential and increased water generation in the fuel cell stack. This led to water adhering to the membrane, causing hydrogen starvation and hindering the passage of protons through the fuel cells. On the other hand, when the purge valve remained closed for longer periods, nitrogen gathered in the anode flow field channel owing to diffusion from the cathode to the anode, resulting in a high nitrogen mass fraction and further hydrogen starvation. At the stable operating stack temperature, the stack voltage gradually decreased during DEA mode. However, as the purge valve was opened, the stack voltage recovered owing to the removal of impurities, water, nitrogen buildup, and the supply of fresh hydrogen.

The stack voltage decay rate was low and not significant at the low load level of 1 A, as depicted in Fig. 7(a). This can be elaborated that the stack operated at a low load level, and the heat generation from the stack was effectively removed by an electric fan, preventing the optimal temperature from being reached. As the load levels increased to 3 A and 5 A, the stack voltage decay rate increased, reaching 1.5 mV and 2.5 mV, respectively, as described in Fig. 7(c) and (e). At the high current level of 8 A, the highest stack voltage decay rate of 5 mV was observed. This phenomenon can be explained by the high stack temperature, which contributed to drying out the membranes owing to the high heat generated by the reaction of electrochemicals in the fuel cell stack. Additionally, water generation caused by back diffusion to the anode side hindered the passage of hydrogen protons from the anode to the cathode. In this study, the average stack voltage reached 13 V, 12 V, 11 V, and 20 V at load levels of 1 A, 3 A, 5 A, and 8 A, respectively. Clearly, as the load levels elevated, the optimal purge interval decreased, as more accumulation of impurities, water, and nitrogen buildup at the anode flow field channel required earlier removal. The step-by-step method was used to examine the effect of purge intervals on the voltage and energy efficiency of the stack. The optimal purge intervals were found to be 540, 360, 280, and 60 s for operating currents of 1 A, 3 A, 5 A, and 8 A, respectively.

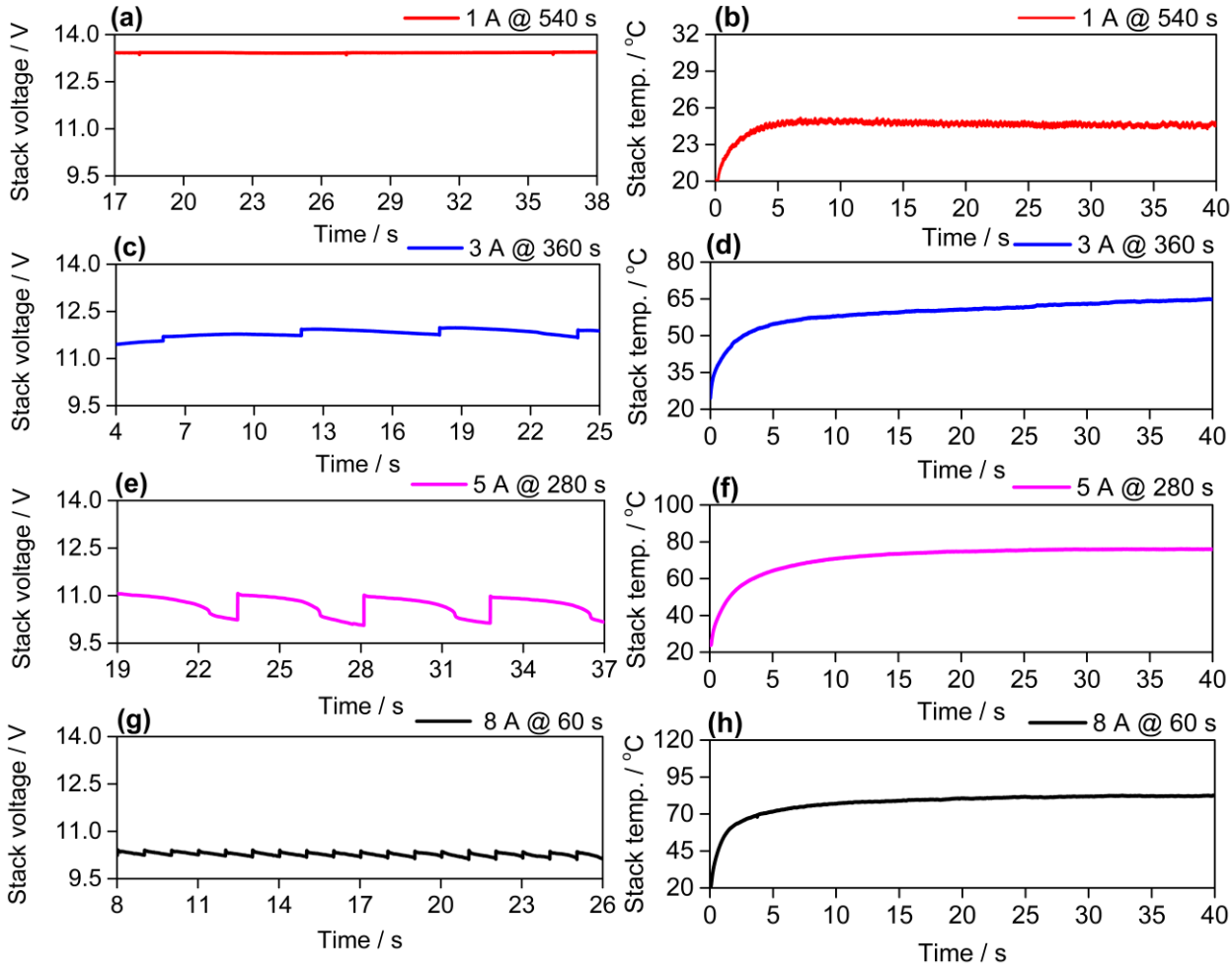

Fig. 7 Voltage of stack performance at stable temperature and stack temperature under various load levels at optimal purge interval

Although the fan's duty cycles were fixed at the optimal value for different purge intervals, the heat generation from the fuel cells varied at different load levels. To clarify the impact of stack temperature on performance, stack temperature was considered and explained under various load levels in this research. The optimal fan's duty cycle was determined in a previous study (Do *et al.* 2024) for various operating load levels. To evaluate the fuel cell stack energy efficiency under different purge intervals, the optimal fan's duty cycle was set to 20% for low and medium operating currents of 1, 3, and 5 A, and 40% for high operating current of 8 A. Fig. 7(b), (d), (f), and (h) show the variation of stack temperature under load levels of 1, 3, 5, and 8 A, respectively. It can be seen that the stack temperature progressively raised from laboratory room temperature to a stable temperature, reaching 35 °C, 50 °C, 67 °C, and 80 °C for load levels of 1, 3, 5, and 8 A, respectively. Clearly, higher load levels resulted in higher stack temperatures owing to the stronger electrochemical reactions occurring in the fuel cell stack.

3.3 Evaluation of stack voltage change and decay rate under different purge intervals

Because the stack was operated under various load levels and purge intervals, the stack voltage performance was dramatically influenced and changed during the DEA configuration. The voltage change and decay rate were determined using Eq. (8) and Eq. (9). The voltage change reflects the susceptibility of the anode channel to flooding, while the voltage decay rate is defined as the average voltage decline per time during each purge cycle (Baumgartner *et al.* 2008).

The variations in voltage change of the PEMFC stack and voltage decay rate of the open-cathode PEMFC stack under varying current levels and purge intervals, as described in Fig. 8(a) and (b), respectively. At a low operating current of 1 A, both voltage change and voltage decay rate remain relatively stable between 180 and 720 s owing to the slow reaction kinetics and slower accumulation of impurities. The voltage decay rate decreased from 0.45 mV s^{-1} to 0.07 mV s^{-1}, allowing for stable cell performance and higher hydrogen utilization at longer purging intervals. However, at higher load levels, both the voltage change of the stack and the voltage decay rate of the stack increased significantly compared to the 1 A case, with a steeper slope corresponding to higher current levels. This indicated that at higher reaction rates, the amount of water generated from the oxygen reduction reaction increases significantly. Consequently, the back diffusion phenomenon from the cathode to the anode, along with nitrogen buildup, leads to adverse conditions such as anode channel flooding and fuel starvation. As membrane resistance increases, the voltage declines sharply, causing both the voltage change of the stack and the voltage decay rate to rise rapidly.

3.4. Fuel cell stack the energy efficiency

The energy efficiency of the stack was evaluated and analyzed under various operating currents and purge intervals in this study. Fig. 9 illustrates the energy efficiency under varying purge intervals and load levels. The energy efficiency

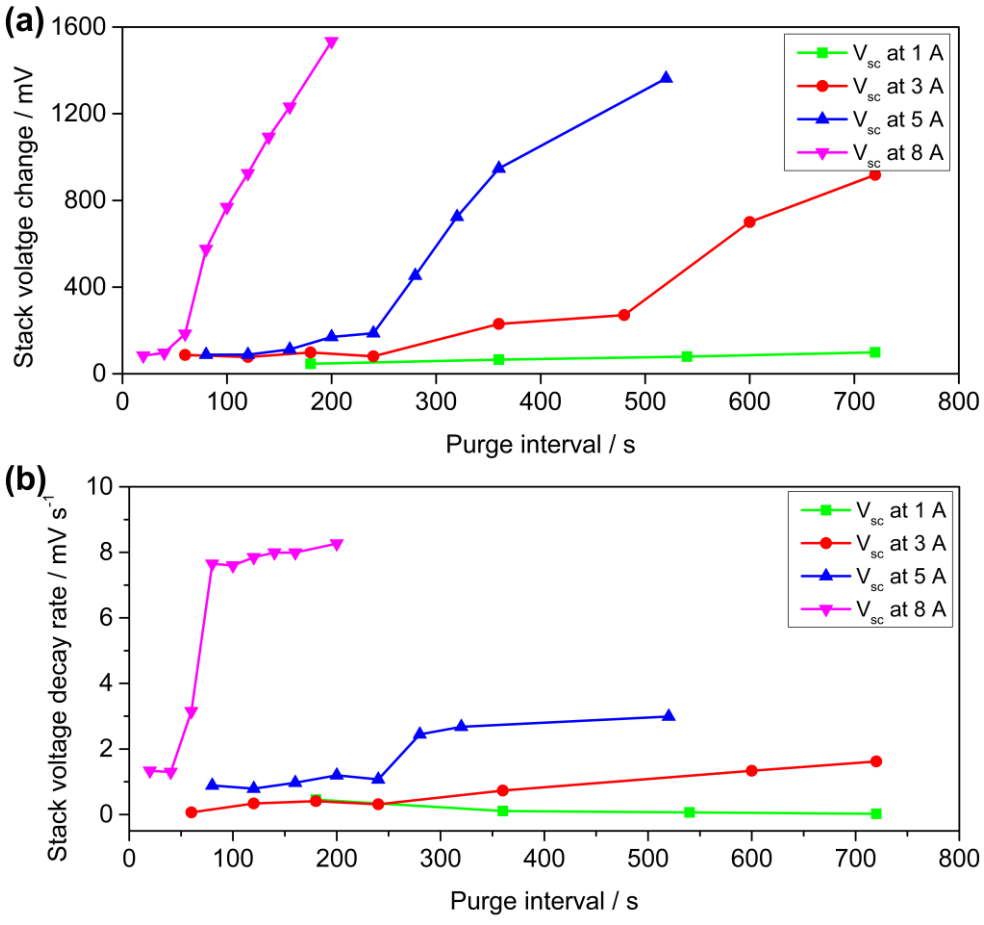

Fig. 8 (a) Voltage change under varying load levels and purge intervals; (b) Voltage decay rate under varying load levels and purge intervals

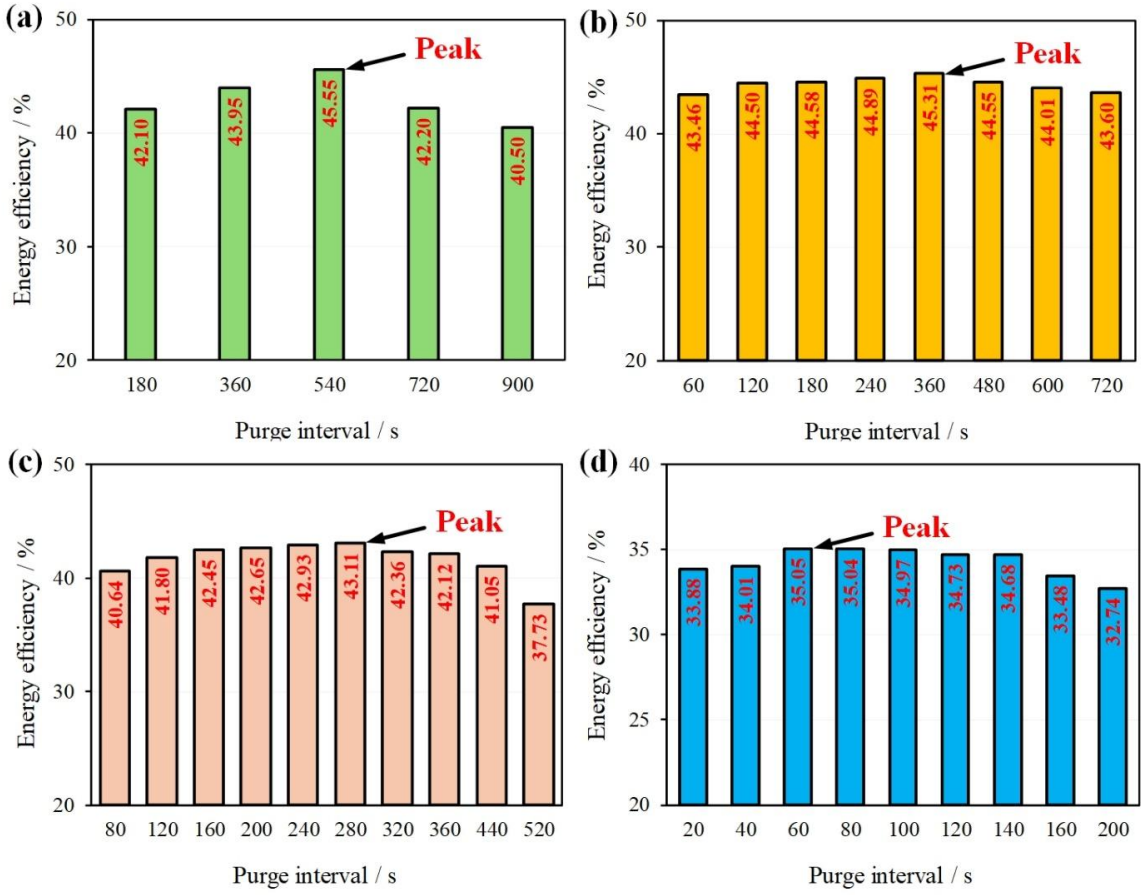

Fig. 9 Energy efficiency under various purge intervals and operating currents: (a) 1 A; (b) 3 A; (c) 5 A; and (d) 8 A

progressively increased to reach its maximum value and then progressively decreased. Additionally, the optimal purge interval was identified at the maximum energy efficiency, as it provided a balance of voltage stability and hydrogen utilization.

At operating currents of 1 A and 3 A, the maximum energy efficiency was achieved at 45.55% and 45.31%, corresponding to optimal purge intervals of 540 s and 360 s. The increase in maximum energy efficiency by 25.22% and 12.91%, respectively, was greater compared to our previous study (Do *et al.* 2024). This is because the stack was operated at the optimal fan's duty cycle, which helped optimize stack temperature and reduce auxiliary power consumption. On the other hand, hydrogen utilization was optimized at the optimal purge intervals. At shorter purge intervals, energy efficiency was lower because more unreacted hydrogen was expelled frequently during the purge valve open phase. Additionally, a reduction in energy efficiency occurred when the purge interval exceeded the optimal point, as the stack voltage deteriorated during longer purge intervals. This led to more water, impurities, and nitrogen buildup at the anode channel, resulting in hydrogen starvation, reduced electrochemical reaction area, and obstruction of fresh hydrogen supply. Furthermore, water attached to the membrane hindered the transport of hydrogen protons from the anode side to the cathode side.

3.5 Hydrogen purge strategy and optimization of energy efficiency

To achieve high energy efficiency, the stack power should remain stable, and the number of purges should be optimized.

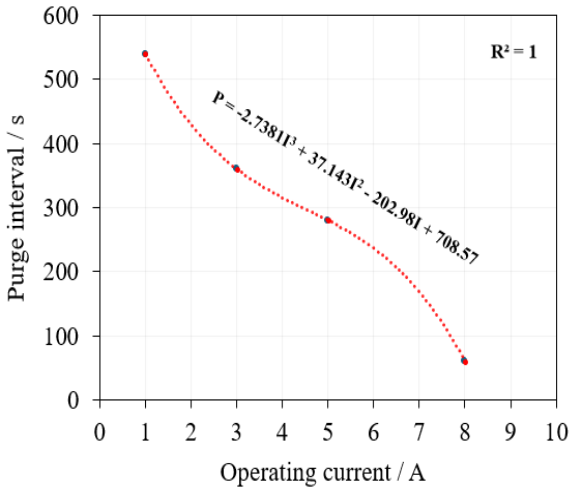

Fig. 10 Hydrogen purge strategy to optimize energy efficiency

Additionally, the power consumption of the auxiliaries, including the electric fan and MCU, should be low. In this study, the highest energy efficiencies achieved were 45.55%, 45.31%, 43.11%, and 35.05%, which represent increases of 25.22%, 12.91%, 9.15%, and 2.09% compared to our previous study (Do *et al.* 2024), corresponding to operating currents of 1, 3, 5, and 8 A. This improvement can be attributed to the optimization of

fan speed, purge intervals, and MCU power consumption in this study. The optimal purge interval was carefully considered, ensuring that the number of purge cycles and voltage stability were reasonable. To find the optimal purge interval, the open-cathode PEMFC stack was investigated under various purge intervals and operating currents using a step-by-step method in this study.

As we all know, as the solenoid valve is closed for a longer time, more water, nitrogen, and impurities build up in the anode flow field channel, increasing the mass transport overpotential. Additionally, a longer purge interval causes hydrogen starvation, leading to a decrease in stack voltage. In contrast, shorter purge intervals result in more unreacted hydrogen being purged frequently. Therefore, the determination of the optimal purge interval for a PEMFC stack is not a straightforward task, as it depends on various factors during stack operation. In practice, the optimal purge interval is considered between hydrogen consumption and voltage stability, which are related to hydrogen utilization and stack power.

In this study, the total operation time of the stack was 2250 s, 1600 s, and 350 s, corresponding to operating currents of 1, 3, 5, and 8 A, respectively. These values were used to determine the total purge time and average voltage degradation under various purge intervals, as detailed in Table 3. To assess the accuracy of the optimal purge interval, trade-off attributes were assigned for different purge intervals and operating currents. These were then used to evaluate and determine the optimal purge interval using a step-by-step method. The optimal purge intervals were found to be 540 s, 360 s, 280 s, and 60 s for operating currents of 1, 3, 5, and 8 A, respectively, as they provided a reasonable balance of voltage stability and hydrogen consumption. Although shorter purge intervals resulted in better voltage stability, which is represented by low average voltage degradation, they also required more frequent purging, leading to a greater amount of unreacted hydrogen being expelled. Longer purge intervals seemed to improve hydrogen utilization, but voltage stability deteriorated due to water, impurities, and nitrogen buildup, which reduced the active electrochemical reaction area.

At the optimal purge intervals across various operating currents, the hydrogen purge strategy was developed in this study, derived from the relationship between purge interval and load levels, as described in Fig. 10. The governing equation was proposed and expressed mathematically in Eq. (14), with high regression and low error.

$$t_{pi} = -2.7381 \times I_{stack}^3 + 37.143 \times I_{stack}^2 - 202.98 \times I_{stack} + 708.57 \quad (14)$$

Where: t_{pi} and I_{stack} represent the purging interval in second (s), and the current level in A, respectively.

This governing equation was programmed and embedded in the MCU to control the purge valve at various load levels, ensuring that the PEMFC stack achieves the highest energy efficiency. Additionally, the current sensor of the stack was employed to determine the load levels and send the signal to the MCU. The MCU then receives the signal from the current sensor, calculates the corresponding purge valve setting for the

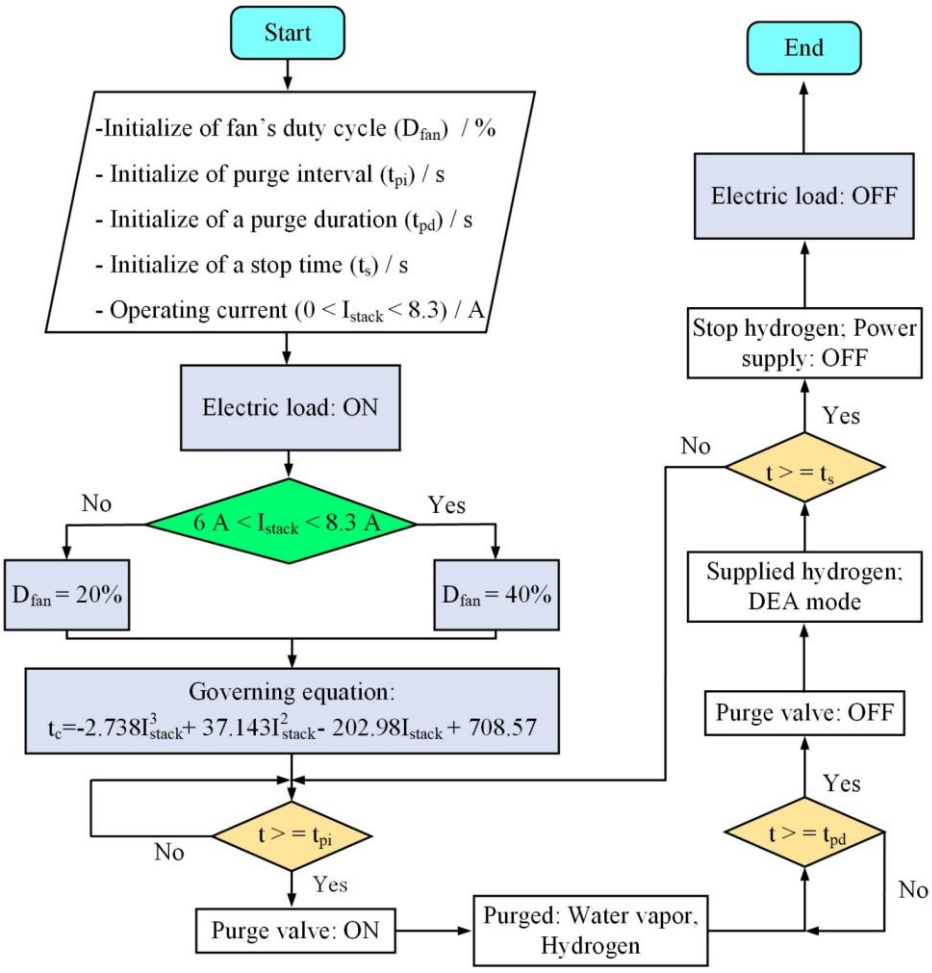

Fig. 11 Strategy for optimizing stack energy efficiency for the open-cathode PEMFC stack in this study

Table 3
Data for evaluating the optimal purge interval, which considers the trade-off between hydrogen utilization and voltage stability for 90 mins

Operating current (A)	Purge interval t_{pi} (s)	Possible maximum number of purging times (N)	Total of pure time τ_p (s)	Average voltage degradation $\overline{V}_d$ (mV)
1	180	30	2.998	45.727
	360	15	1.500	65.012
	540	10	1.000	78.951
	720	7	0.750	99.262
	900	6	0.600	114.351
3	60	90	8.985	86.923
	180	30	2.998	98.679
	360	15	1.500	229.944
	480	11	1.125	270.621
	720	7	0.750	918.025
5	80	67	6.742	88.402
	160	34	3.373	112.617
	280	19	1.928	452.805
	360	15	1.500	947.099
	520	10	1.038	1363.165
8	20	269	26.866	83.405
	40	135	13.466	96.148
	60	90	8.985	184.382
	100	54	5.395	768.761
	140	39	3.854	1092.683

load level, and subsequently sends the control signal to regulate the purge valve. This process aims to maintain maximum energy efficiency as the load levels of the stack change, with the control system adapting to optimize energy efficiency.

In this study, the hydrogen purge strategy to optimize energy efficiency is described in detail in the flowchart of Fig. 11. The parameter inputs include the optimal fan's duty cycle, purge duration, limiting operating current, and duration of the stack, all of which were set up in the MCU. The current sensor was used to measure the load level of the stack. If the load level of the stack is less than 6 A, the optimal fan's duty cycle of 20% is used. On the other hand, if the load level ranges from 6 to 10 A, the optimal fan's duty cycle of 40% is selected to optimize stack temperature and reduce fan power consumption. Next, the purge interval corresponding to the load level is determined. The stack operates in a dead-end anode configuration, with the purge valve being opened and closed according to the MCU control.

4. Conclusion

The DEA configuration was investigated under various operating currents and purge intervals at the optimal fan speed in this study. Additionally, a hydrogen purge strategy for the open-cathode PEMFC stack in DEA mode was developed to optimize energy efficiency. Several interesting conclusions were revealed in this study. As the load levels of the fuel cell stack increased, the voltage of the stack decreased due to higher overpotential and increased heat generation. Additionally, the stack voltage declined with longer purge intervals because more water, impurities, and nitrogen buildup gathered in the anode flow field channel, resulting in a reduced effective activation electrochemical area. With short purge intervals, the stack voltage remained stable because the purge valve was opened frequently, expelling water, impurities, and nitrogen, leading to prompt performance recovery. However, this also resulted in increased hydrogen waste. Therefore, the optimal purge interval in this study was determined by balancing stable voltage and hydrogen consumption. The open-cathode PEMFC stack energy efficiency was determined under varying load levels and purge intervals. The energy efficiencies achieved were 45.55%, 45.31%, 43.11%, and 35.05%, which represent increases of 25.22%, 12.91%, 9.15%, and 2.09%, respectively, compared to the previous study, corresponding to operating currents of 1, 3, 5, and 8 A. This improvement can be attributed to the optimization of the fan's speed, purge interval, and MCU power consumption in this study. In addition, the optimal purge interval decreased as the operating current increased because more water, impurities, and nitrogen buildup at the anode channel needed to be removed earlier. Finally, the hydrogen purge strategy was optimized to achieve the highest energy efficiency with the optimal purge interval and the fan's duty cycle. The governing equation was provided. This strategy is significant for optimizing hydrogen consumption and maintaining stable stack voltage.

Abbreviations and nomenclatures

D_{fan}	Electric fan duty cycle
DC	Direct current
DAQ	Data Acquisition
DEA	Dead-end anode
F	Faraday's constant ($F = 96485\ C\ mol^{-1}$)
i	Summation index
I_{stack}	Operating stack current level (A)
I_{aux}	Auxiliary current (A)
K_v	Purge valve characteristic
LHV	Hydrogen's lower heating value ($LHV = 241\ kJ\ mol^{-1}$)
MCU	Microcontroller Unit
$MAPE$	Mean absolute percentage error
n	Cell number in the stack
N	Possible maximum purging times number
p_a	Anode inlet pressure (atm)
p_0	Anode outlet pressure (atm)
PEMFCs	Proton exchange membrane fuel cells
PWM	Pulse width modulation
P_{net}	Net power output (W)
P_{stack}	Power of the open-cathode fuel cell stack (W)
P_{aux}	Power of the auxiliary (W)
P_{pv}	Power consumption of the purge valve (W)
P_{Hsp}	Power consumption of the hydrogen supply valve (W)
P_{Fan}	Power consumption of the electric fan (W)
P_{MCU}	Power consumption of the MCU (W)
t_{pi_e}	Purge interval from the experiment (s)
t_{pi_p}	Purge interval from the proposal in this study (s)

t_{pp}	Purge period (s)
t_{pi}	Purging interval (s)
t_{pd}	Purge duration (s)
τ_p	Total of pure time possible maximum
T_{on}	Pulse width time (s)
T_{cycle}	Period time of one cycle (s)
T_{stack}	Stack temperature (K)
UUVs	Unmanned underwater vehicles
UAVs	Unmanned aerospace vehicles
$\dot{v}_{H_2}$	Volume of hydrogen flow rate, in litter per minutes (LPM)
$\dot{v}_{H_{2,fc}}$	Flow rate of the hydrogen consumption for the electrochemical reaction of the stack (LPM)
$\dot{v}_{H_{2,pp}}$	Wasted hydrogen consumption flow rate owing to the purging process (LPM)
V_{stack}	Stack voltage (V)
V_{aux}	Auxiliary voltage (V)
V_{sc}	Stack voltage change (V)
V_{dc}	Stack voltage decay rate (V s^{-1})
$\bar{V}_d$	Average voltage degradation (mV)
$V_{t_{ap}^i}$	Stack voltage in mV (after previous purging) at the beginning of the new cycle (i+1)th (s)
$V_{t_{bp}^{i+1}}$	Stack voltage (before next purging) at the end of the (i+1)th cycle (s)
Δt_{fc}	Total of open-cathode PEMFC stack operation time (s)
η_{LHV}	Energy efficiency of the fuel cell stack
ρ	Density of hydrogen (kg m^{-3})

Acknowledgments

The first and second authors would like to thank Lac Hong University for financial support. The last author would like to thank Mechanical Engineering Department, National Chung Cheng Unviersity for providing experimental equipment and the (Taiwan Experience Education Program-TEEP), Taiwan, Republic of China (R.O.C.), for supporting this study during the internship period.

Author Contributions: T.T.D.: Conceptualisation; Methodology; Validation; Investigation; Formal analysis; Data curation; Software; Writing - original draft; Writing - review & editing; Funding acquisition; Project administration; Supervision, T.K.V.; Investigation; Resources; Software; Visualisation; Writing - original draft, P.D.D.; Validation; Investigation; Data curation; Software; Writing - original draft. All authors have read and agreed to the published version of the manuscript.

Conflicts of Interest: The authors declare no conflict of interest.

Data availability: Data will be made available on request.

References

Abbou, S., Dillet, J., Spernjak, D., Mukundan, R., Borup, R. L., Maranzana, G., & Lottin, O. (2015). High potential excursions during PEM fuel cell operation with dead-ended anode. *Journal of The Electrochemical Society,* 162(10), F1212-F1220. https://doi.org/10.1149/2.0511510jes

Abdelkareem, M. A., Elsaid, K., Wilberforce, T., Kamil, M., Sayed, E. T., & Olabi, A. (2021). Environmental aspects of fuel cells: A review. *Science of The Total Environment,* 752, 141803. https://doi.org/10.1016/j.scitotenv.2020.141803

Ahluwalia, R. K., and X. Wang. (2007). Buildup of nitrogen in direct hydrogen polymer-electrolyte fuel cell stacks. *Journal of Power Sources,* 171(1), 63–71. https://doi.org/10.1016/j.jpowsour.2007.01.032

Baik, Kyung-Don, and Min-Soo Kim. (2011). Characterization of nitrogen gas crossover through the membrane in proton-exchange membrane fuel cells. *International Journal of Hydrogen Energy*, 36(1), 732–739. https://doi.org/10.1016/j.ijhydene.2010.09.046

Baik, Kyung-Don, and Min-Soo Kim. (2008). Characterization of Nitrogen Gas Crossover in PEM Fuel Cell Stacks. Proceedings of the KSME Conference, *The Korean Society of Mechanical Engineers,*. https://doi.org/10.3795/KSME-B.2009.33.3.207

Barbir, F. (2012). PEM fuel cells: Theory and practice. Academic Press, ISBN: 9780123877109

Baumgartner, W. R., Parz, P., Fraser, S. D., Wallnöfer, E., & Hacker, V. (2008). Polarization study of a PEMFC with four reference electrodes at hydrogen starvation conditions. *Journal of Power Sources,* 182(2), 413-421. https://doi.org/10.1016/j.jpowsour.2008.01.001

Baz, F. B., Elzohary, R. M., Osman, S., Marzouk, S. A., & Ahmed, M. A (2024). Review of water management methods in proton exchange membrane fuel cells. *Energy Conversion and Management,* 302 , 118150. https://doi.org/10.1016/j.enconman.2024.118150

Chen, J., Sun, L., Zhu, W., Pei, H., Xing, L., & Tu, Z. (2024). Influence of cathode air supply mode on the performance of an open cathode air-cooled proton exchange membrane fuel cell stack. *Applied Thermal Engineering,* 243, 122709. https://doi.org/10.1016/j.applthermaleng.2024.122709

Chen, J., Siegel, J. B., Stefanopoulou, A. G., & Waldecker, J. R. (2013). Optimization of purge cycle for dead-ended anode fuel cell operation. *International Journal of Hydrogen Energy*, 38(12), 5092–5105. https://doi.org/10.1016/j.ijhydene.2013.02.022

Do, T. T., Chen, Y. S., Ly, V. D., Huynh, P. S., Nguyen, V. T., & Le, P. L. (2024, July). Study on the Effect of Fan Speed on the Energy Efficiency of an Open Cathode PEMFC with Wi-Fi Protocol. *In 2024 7th International Conference on Green Technology and Sustainable Development (GTSD)* (pp. 320-325). IEEE. https://doi.org/10.1109/GTSD62346.2024.10675189

Guo, Z., Tian, C., Gong, K., Xu, W., Chen, L., & Tao, W. Q. (2024). Experimental study on the dynamic response of voltage and temperature of an open-cathode air-cooled proton exchange membrane fuel cell. *International Journal of Hydrogen Energy*, 57, 601-615. https://doi.org/10.1016/j.ijhydene.2024.01.045

Hu, Z., YiYu, Wang, G., Chen, X., Chen, P., Chen, J., & Zhou, S. Anode purge strategy optimization of the polymer electrode membrane fuel cell system under the dead-end anode operation. *Journal of Power Sources,* 320 (2016): 68–77. https://doi.org/10.1016/j.jpowsour.2016.04.023

Kandidayeni, M., Macias, A., Boulon, L., & Kelouwani, S. (2019). Efficiency enhancement of an open cathode fuel cell through a systemic management. *IEEE Transactions on Vehicular Technology,* 68(12), 11462-11472. https://doi.org/10.1109/TVT.2019.2944996

Khokhar, Hassan Naeem. (2023). Decarbonisation of Global Economies; Is Net Zero Emission Achievable? The Case for Hydrogen and Fuel Cell Technology for Innovative Futures. *Journal of Entrepreneurship and Innovation in Emerging Economies*, 9(1) , 92–130. https://doi.org/10.1177/23939575221141578

Kocha, Shyam S., J. Deliang Yang, and Jung S. Yi. (2006). Characterization of gas crossover and its implications in PEM fuel cells. *AIChE Journal,* 52(5) (2), 1916–1925. https://doi.org/10.1002/aic.10780

Kurniaa, J. C., Sasmito, A. P., & Shamimc, T. (2019). Advances in proton exchange membrane fuel cell with dead-end anode operation: A review. *Applied Energy,* 252, 113416. https://doi.org/10.1016/j.apenergy.2019.113416

Lee, J., Ko, S., Kim, B. K., Ryu, J. H., Baek, J. D., & Kang, S. W. (2024). Empirical lifetime prediction through deterioration evaluation of high-power PEMFC for railway vehicle applications. International *Journal of Hydrogen Energy*, 71, 972-981. https://doi.org/10.1016/j.ijhydene.2024.05.185

Lee, Y., Kim, B., & Kim, Y. (2009). An experimental study on water transport through the membrane of a PEFC operating in the dead-end mode. *International Journal of Hydrogen Energy*, 34(18), 7768–7779. https://doi.org/10.1016/j.ijhydene.2009.07.010

Li, Q., Sun, K., Suo, M., Zeng, Z., Guan, C., Liu, H., ... & Wang, T. (2024). Water transport in PEMFC with metal foam flow fields: Visualization based on AI image recognition. *Applied Energy,* 365, 123273. https://doi.org/10.1016/j.apenergy.2024.123273

Liu, Y., Zhang, W., Lei, J., Deng, X., & Liu, Y. (2026). Anode internal purge (AIP) technique for the co-optimization of system efficiency and stack reliability in air-cooled PEMFCs. *Fuel,* 417, 138641. https://doi.org/10.1016/j.fuel.2026.138641

Ling, C. Y., Cao, H., Chen, Y., Han, M., & Birgersson, E. (2016). Compact open cathode feed system for PEMFCs. *Applied Energy*, 164, 670-675. https://doi.org/10.1016/j.apenergy.2015.12.012

Manokaran, A., Pushpavanam, S., Sridhar, P., & Pitchumani, S. (2011). Experimental analysis of spatio-temporal behavior of anodic dead-end mode operated polymer electrolyte fuel cell. *Journal of Power Sources,* 196(23), 9931-9938. https://doi.org/10.1016/j.jpowsour.2011.06.103

Meyer, Q., Ashton, S., Torija, S., Gurney, C., Boillat, P., Cochet, M., ... & Brett, D. J. (2016). Nitrogen blanketing and hydrogen starvation in dead-ended-anode polymer electrolyte fuel cells revealed by hydro-electro-thermal analysis. *Electrochimica Acta,* 203, 198-205. https://doi.org/10.1016/j.electacta.2016.04.018

Meyer, Q., Ashton, S., Curnick, O., Reisch, T., Adcock, P., Ronaszegi, K., ... & Brett, D. J. (2014). Dead-ended anode polymer electrolyte fuel cell stack operation investigated using electrochemical impedance spectroscopy, off-gas analysis and thermal imaging. *Journal of Power Sources*, 254, 1-9. https://doi.org/10.1016/j.jpowsour.2013.11.125

Mokmeli, A., & Asghari, S. (2010).An investigation into the effect of anode purging on the fuel cell performance. *Journal of Fuel Cell Science and Technology,* 35(17), 9276–9282. https://doi.org/10.1016/j.ijhydene.2010.03.079

Müller, E. A., Kolb, F., Guzzella, L., Stefanopoulou, A. G., & McKay, D. A. (2010). Correlating nitrogen accumulation with temporal fuel cell performance. *J. Fuel Cell Sci. Technol.* 7(2), 021013 https://doi.org/10.1115/1.3177447

Mus, J., Nuyttens, R., Vanierschot, M., Vandeginste, V., & Buysschaert, F. (2025). Experimental study of the effects of ambient conditions on the performance of open-cathode PEM fuel cells. *Journal of Power Sources,* 660, 238467. https://doi.org/10.1016/j.jpowsour.2025.238467

Ohs, J. H., Sauter, U., Maass, S., & Stolten, D. (2011). Modeling hydrogen starvation conditions in proton-exchange membrane fuel cells. Journal of Power Sources, 196(1), 255-263. https://doi.org/10.1016/j.jpowsour.2010.06.038

O'hayre, R., Cha, S. W., Colella, W., & Prinz, F. B. (2016). Fuel cell fundamentals. John Wiley & Sons.

Paul, Biddyut, and John Andrews. (2017). PEM unitised reversible/regenerative hydrogen fuel cell systems: State of the art and technical challenges. *Renewable and Sustainable Energy Reviews,* 79, 585–599. https://doi.org/10.1016/j.rser.2017.05.112

Pei, H., Xiao, C., & Tu, Z. (2022). Experimental study on liquid water formation characteristics in a novel transparent proton exchange membrane fuel cell. *Applied Energy*, 321 , 119349. https://doi.org/10.1016/j.apenergy.2022.119349

Rahimi-Esbo, M., A. A. Ranjbar, and S. M. Rahgoshay. (2020). Analysis of water management in PEM fuel cell stack at dead-end mode using direct visualization. *Renewable Energy,* 162, 212–221. https://doi.org/10.1016/j.renene.2020.06.078

Sasmito, A. P., Birgersson, E., Lum, K. W., & Mujumdar, A. S. (2012). Fan selection and stack design for open-cathode polymer electrolyte fuel cell stacks. *Renewable Energy*, 37(1), 325-332. https://doi.org/10.1016/j.renene.2011.06.037

Sezgin, B., Devrim, Y., Ozturk, T., & Eroglu, I. (2022). Hydrogen energy systems for underwater applications. *International Journal of Hydrogen Energy,* 47(45), 19780-19796. https://doi.org/10.1016/j.ijhydene.2022.01.192

Shi, L., Du, C., Zhou, J., Yi, Y., Li, R., Liu, Z., ... & Tang, X. (2025). Optimization of fuel cell shutdown purge strategy based on machine learning: Mechanism analysis and experimental verification. *Renewable Energy,* 248, 123165. https://doi.org/10.1016/j.renene.2025.123165

Song, Y., Zhang, C., Deshpande, A., Tan, K., & Han, M. (2020). Fixed air flow-rate selection by considering the self-regulating function of low power air-cooled PEMFC stack. *International Journal of Heat and Mass Transfer,* 158, 119771. https://doi.org/10.1016/j.ijheatmasstransfer.2020.119771

Van Biert, L., Godjevac, M., Visser, K., & Aravind, P. V. (2016). A review of fuel cell systems for maritime applications. *Journal of Power Sources,* 327, 345-364. https://doi.org/10.1016/j.jpowsour.2016.07.007

Wang, B., Zhao, D., Li, W., Wang, Z., Huang, Y., You, Y., & Becker, S. (2020). Current technologies and challenges of applying fuel cell hybrid propulsion systems in unmanned aerial vehicles. *Progress in Aerospace Sciences,* 116, 100620. https://doi.org/10.1016/j.paerosci.2020.100620

Wang, Wen Cheng. (2010). A speed regulation system of DC motor based on PWM technology. *Applied Mechanics and Materials*, 29, 2194–2199. https://doi.org/10.4028/www.scientific.net/AMM.29-32.2194

Wilberforce, T., Alaswad, A., Palumbo, A., Dassisti, M., & Olabi, A. G. (2016). Advances in stationary and portable fuel cell applications. *International journal of hydrogen energy*, 41(37), 16509-16522. https://doi.org/10.1016/j.ijhydene.2016.02.057

Wilberforce, T., El-Hassan, Z., Khatib, F. N., Al Makky, A., Baroutaji, A., Carton, J. G., & Olabi, A. G. (2017). Developments of electric cars and fuel cell hydrogen electric cars. *International Journal of Hydrogen Energy,* 42(40), 25695-25734. https://doi.org/10.1016/j.ijhydene.2017.07.054

Xu, K., Chen, D., Guo, R., Chang, K., Hu, S., Pei, P., & Xu, X. (2025). Control and purge strategies for hydrogen supply subsystem of proton exchange membrane fuel cell system. *International Journal of Hydrogen Energy,* 149, 150050. https://doi.org/10.1016/j.ijhydene.2025.150050

Xiao, F., Chen, T., Chen, Z., Lan, Y., Zhang, S., & Liu, S. (2025). The study on the performance of air-cooled open-cathode PEMFC with dead-ended anode. *International Journal of Green Energy,* 22(3), 570-581. https://doi.org/10.1080/15435075.2024.2421332

Yang, Y., Zhang, X., Guo, L., & Liu, H. (2020). Local degradation in proton exchange membrane fuel cells with dead-ended anode. *Journal of Power Sources,* 477 , 229021. https://doi.org/10.1016/j.jpowsour.2020.229021

Yang, H., Yin, C., Tan, Y., Xu, Y., & Tang, H. (2025). Anode nitrogen content estimation and purge strategy optimization of fuel cell system. *Applied Energy,* 399, 126463. https://doi.org/10.1016/j.apenergy.2025.126463

Yu, J., Jiang, Z., Hou, M., Liang, D., Xiao, Y., Dou, M., Shao, Z., & Yi, B. (2014). Analysis of the behavior and degradation in proton exchange membrane fuel cells with a dead-ended anode. *Journal of Power Sources,* 246. 90–94. https://doi.org/10.1016/j.jpowsour.2013.06.163

Yu, X., Zhang, C., Li, M., Chen, B., Fan, M., Sheng, X., & Ma, F. (2023). Experimental investigation of self-regulating capability of open-cathode PEMFC under different fan working conditions. *International Journal of Hydrogen Energy*, 48(68), 26599-26608. https://doi.org/10.1016/j.ijhydene.2022.06.027

Yu, X., Zhang, C., Li, M., Wang, G., Tu, Z., Yu, T., ... & Zhao, F. (2024). Thermal management of an open-cathode PEMFC based on constraint generalized predictive control and optimized strategy. *Renewable Energy,* 220, 119608. https://doi.org/10.1016/j.renene.2023.119608

Zeng, T., Zhang, C., Huang, Z., Li, M., Chan, S. H., Li, Q., & Wu, X. (2019). Experimental investigation on the mechanism of variable fan speed control in Open cathode PEM fuel cell. *International Journal of Hydrogen Energy,* 44(43), 24017-24027. https://doi.org/10.1016/j.ijhydene.2019.07.119

Zhao, C., Xing, S., Liu, W., & Wang, H. (2021). Air and H2 feed systems optimization for open-cathode proton exchange membrane fuel cells. *International Journal of Hydrogen Energy*, 46(21), 11940-11951. https://doi.org/10.1016/j.ijhydene.2021.01.044

Zhou, J., Zhifei, F., and Huichao, D.. (2023). Effect of Fan Parameters on Forced-Convection Open-Cathode Proton Exchange Membrane Fuel Cells. *World Hydrogen Technology Convention. Singapore: Springer Nature Singapore.* https://doi.org/10.1007/978-981-99-8631-6_42